

Sonderdruck aus:

BOREAS

MÜNSTERSCHE BEITRÄGE ZUR ARCHÄOLOGIE

Begründet von Werner Fuchs

Herausgegeben von Dieter Korol, Achim Lichtenberger,
Dieter Salzmann, Magdalene Söldner, Klaus Stähler

Redaktion: Sophia Nomicos unter Mitarbeit von Vanessa Galk und Max Römelt



Band 45/46
Münster 2022/2023

Gedruckt mit Unterstützung durch den Landschaftsverband Westfalen-Lippe,
Abteilung Kulturpflege



Für die Menschen.
Für Westfalen-Lippe.

und das Ministerium für Wirtschaft, Energie, Bauen, Wohnen und Verkehr
des Landes Nordrhein-Westfalen

BOREAS - Münstersche Beiträge zur Archäologie 45/46, 2022/2023

Herausgebende: Dieter Korol, Achim Lichtenberger, Dieter Salzmann, Magdalene Söldner, Klaus Stähler

Redaktion: Sophia Nomicos unter Mitarbeit von Vanessa Galk und Max Römelt, Institut für Klassische Archäologie und Christliche Archäologie/Archäologisches Museum, Domplatz 20–22, 48143 Münster
Satz und Umbruch: Lianna Hecht

Zu beziehen durch: Scriptorium, Trappweg 12, 34431 Marsberg/Padberg. Telefon: 02991-908773,
Fax 02991-908774, E-Mail: info@scriptorium-muenster.de, Internet: www.scriptorium-muenster.de

Austauschangebote sind zu richten an die Herausgebenden des Boreas, Institut für Klassische Archäologie und Christliche Archäologie/Archäologisches Museum, Domplatz 20–22, 48143 Münster

E-Mail: inst.arch@uni-muenster.de

Dieses Werk ist urheberrechtlich geschützt. Die dadurch begründeten Rechte, insbesondere die der Übersetzung, des Nachdrucks, der Entnahme von Abbildungen, der Funksendung, der Wiedergabe auf fotomechanischem oder ähnlichem Wege und der Speicherung in Datenverarbeitungsanlagen bleiben, auch bei nur auszugsweiser Verwertung, vorbehalten. Das Einstellen von Sonderdrucken auf Plattformen wie academia.edu oder ähnlichen Einrichtungen ist nur mit ausdrücklicher Zustimmung des Verlages vor Ablauf von zwei Jahren nach Erscheinen des Bandes erlaubt. Die Vergütungsansprüche des § 54, Abs. 2, UrhG, werden durch die Verwertungsgesellschaft Wort wahrgenommen.

ISBN 978-3-932610-68-4



Im Gedenken an

Prof. Dr. Dr. h.c. Hugo Brandenburg (13.06.1929 – 26.12.2022),
Universitätsprofessor für Klassische Archäologie mit besonderer Berücksichtigung
der Spätantike an der Universität Münster (1.10.1982 – 31.07.1994)
sowie Mitherausgeber des „Boreas. Münstersche Beiträge zur Archäologie“

Inhalt

OLAF DÖRRER

Zum Beginn der ›hoplitischen‹ Bewaffnung in Griechenland..... 1

ACHIM LICHTENBERGER

Pheidias, Homer and Olympus. On Helios and Selene framing scenes in the Parthenon
and in Olympia 19

SYUZANNA MURADYAN

Zum Nachleben urartäischer Architektur im Jerwandaschat-Komplex am Araxes (Armenien)... 45

MICHAEL DONDERER

Zu einer Gruppe von Mosaiken mit Darstellungen der Jahreszeiten.
Folgerungen aus ihrem Gliederungsschema 65

KLAUS FITTSCHEN

Lesefrüchte IX..... 95

KLAUS FITTSCHEN

Lesefrüchte X. Nicht von Cavaceppi, antik! Zu den Büsten der Faustina minor
und einer unbekanntenen Frau (›Faustina maior‹) in der Ermitage in St. Petersburg..... 115

ACHIM LICHTENBERGER – TORBEN SCHREIBER – MKRTICH H. ZARDARYAN

The Armenian-German Artaxata Project:
Preliminary Report on the Excavations in Artashat 2021 121

ACHIM LICHTENBERGER – TORBEN SCHREIBER – MKRTICH H. ZARDARYAN

Armenian-German Artaxata Project:
Preliminary Report on the Excavations in Artashat 2022 169

SOPHIA NOMICOS – STAVROS VLIZOS – MICHAEL BECKEN – ANASTASIOS KAZOLIAS –

VAYIA PANAGIOTIDIS – VOLKMAR SCHMIDT – MORITZ WENDEL – NIKOLAOS ZACHARIAS

Remote Sensing and Geophysical Survey at the Sanctuary of Apollo Amyklaios, Sparti, Greece.
Results of the 2022 Measurements..... 217

Aus Westfalen

OLIVER BREHM

Die Sammlung Wegner im Archäologischen Museum der Universität Münster (Teil 1) 249

OLIVER BREHM

Ex ungue leonem - Die figürlich verzierte Attasche eines Kohlenbeckens 281

**ACHIM LICHTENBERGER - H.-HELGE NIESWANDT - LAURA STUTENBECKER -
DAVID DE VLEESCHOUWER**

Das Porträt eines Mannes von einem kaiserzeitlichen Grabrelief aus Thessaloniki.

Provenienzforschung im Archäologischen Museum der Universität Münster 297

Adressen der Autorinnen und Autoren 311

Hinweise für Autorinnen und Autoren des BOREAS 313

SOPHIA NOMICOS, STAVROS VLIZOS, MICHAEL BECKEN, ANASTASIOS KAZOLIAS,
VAYIA PANAGIOTIDIS, VOLKMAR SCHMIDT, MORITZ WENDEL, NIKOLAOS ZACHARIAS

Remote Sensing and Geophysical Survey at the Sanctuary of Apollo Amyklaios, Sparti, Greece. Results of the 2022 Measurements

ABSTRACT

Archaeological research at the sanctuary of Apollo at Amyklai goes back to the 19th century with a long history of excavation within the peribolos. There is, however, still little research on the use of the adjacent areas of the temenos, although according to the literary evidence, the Hyakinthia festival extended to areas outside of the core of sanctuary. The aims of this study were to investigate the immediate surroundings of the sanctuary for evidence of anthropogenic use, thereby identifying potential zones for excavation and to better understand the topographical features of the site. To achieve this, we employed the geophysical methods of magnetic surveying and susceptibility measurements, electrical resistivity tomography (ERT) and ground-penetrating radar (GPR) as well as close-range aerial photogrammetry and LiDAR scanning (also known as airborne laser scanning or ALS). The results of the different methods suggest human activity in the investigated areas, the exact nature of which will have to be clarified by targeted excavations.

INTRODUCTION

The archaeological site of the sanctuary of Apollo Amyklaios is located on the hill of Agia Kyriaki approximately 6 km south of Sparta, east of the main road connecting the modern city with the coastal town of Gytheion on the Laconian Gulf. As one of several hills, it overlooks the fertile northern plain of the Eurotas valley between the two dominant southern Peloponnesian Mountain ranges of Taygetos and Parnon (Fig. 1)¹.

Famous in Antiquity for the unique architectural monument, the ›Throne of Apollo‹, and the Hyakinthia games, »the Panathenaic Games of the Spartans«², the sanctuary was one of the main cult sites of the Spartans³. On his way through Lakonia, Pausanias (Paus. 3,19,2) visited the site and informs us in detail about the building that housed the statue of Apollo. The monument was supposedly built by the Ionian architect Bathykles during the late archaic period, which attests once more for the close connections Sparta held with the cities of Asia Minor⁴. In terms of ancient topography, the sanctuary was located at Amyklai, a place

¹ Polybius (Pol. 5,19,2) cited Amyklai as one of the most richly timbered and fertile areas in Laconia, which is also confirmed by the present state of the landscape.

² Cf. Welwei 2013, 31. On this topic see especially Brulé 1992.

³ On the ›Throne‹ see Martin 1987; Förtsch 2001, 81–2; Delivorrias 2009; Bilis and Magnisali 2011–2012, 131 f., fig. 6. On the Hyakinthia see Petterson 1992, 9–10; Calame 1997, 174–185; Larson 2007, 91; Parker 2011, 188–190; Richer 2012, 343–382; Petropoulou 2015; Vlachou 2017; Vlachou 2018.

⁴ Regarding the Asia Minor-Ionian influences in Spartan art, see Rolley 1977, 132; Prost 2018, 168–169.



Fig. 1: Aerial photo of Agia Kyriaki Hill from south-east (Amykles Research Project).



Fig. 2: Stamped rooftile from 2023 excavation (Amykles Research Project).

already mentioned in Homer's catalogue of ships in the *Iliad* (Hom. Il. 2,584). According to tradition, the town, which has not yet been identified in the modern topography, was at some point incorporated by Sparta in an act of synoecism⁵.

Already in the 19th century, the site of Agia Kyriaki was identified as the sanctuary where Apollo Amyklaios and the mythological figure of Hyakinthos were worshipped in Antiquity⁶. This has been confirmed over the years by finds of stamped roof tiles bearing the words of Apollo Amyklaios or variations of this (Fig. 2)⁷. The site was excavated several times since the 19th century: After a first investigation by Chr. Tsountas in 1890, it was researched by German archaeologists E. Fiechter (1905) and E. Buschor (1925)⁸. In the 1960s small-scale excavations were carried out by the late A. Delivorrias, who revived his efforts in 2005 with the inauguration of systematic excavations on the hill⁹. The project which has been running for nearly twenty years, is now being directed by S. Vlizon under the Auspices of the Archaeological Society of Athens. While the initial focus of the project lay on the reconstruction of the ›Throne‹ monument, over the course of the years a number of new structures have been revealed, and it has thus become possible to obtain a clearer picture of the chronology and the infrastructure of the site¹⁰.

It can now be substantiated that the earliest evidence of human activity on the site dates back to the Early Helladic Period when a settlement which continued into the Middle Helladic Period was established¹¹. The hill was transformed into a sanctuary during the Mycenaean Period, linking it to the famous Vapheio tomb and other Mycenaean remains in the area¹². A large number of Geometric sherds attest to cultic activity throughout all phases of the Geometric period¹³. In accordance with the literary evidence, the results of the excavation confirm major building activity in the late archaic period, when the massive peribolos wall, the ›Throne‹ monument, the circular altar as well as a propylon were erected¹⁴.

While there is evidence for Classical, Hellenistic and Roman activity, it is the late Roman / Early Byzantine phase that has left another major imprint on the site. The first Christian Basilica was erected on the hill in the Early Byzantine Period, and the church of Agia Kyriaki which is now standing on the hill dates to the 19th century¹⁵.

⁵ RE I,2 (1894) 1996 f. s. v. Amyklai (G. Hirschfeld); Tosti 2020.

⁶ Matalas 2011–2012.

⁷ Tsountas 1892, 3; Buschor – von Massow 1927, 64.

⁸ Fiechter 1905; Buschor – von Massow 1927; Vlizon 2019.

⁹ Vlizon 2011–2012.

¹⁰ Vlizon 2017; Vlizon 2020.

¹¹ Buschor – von Massow 1927, 3–10; Vlizon 2010a, 579; Vlizon 2010b, 244–245.

¹² See Demakopoulou 2009a; Demakopoulou 2009b; Demakopoulou 2011–2012.

¹³ Vlachou 2017; Vlachou 2018.

¹⁴ Vlizon 2017.

¹⁵ On the later phases see Tsountas 1892. Results of the current project and new interpretation on this subject were presented at the international symposium ›From Sparta to Lacedaemon: daily lifeways of a Byzantine city‹ organized by the British School at Athens on May 3rd 2023.

Although the relative chronology of the life of the site can now be outlined with some clarity, the position of the sanctuary within its local and regional context still remains unexplored. Neither the relationship between the hitherto unlocated settlement of Amyklai nor the role of the immediate surrounding of the sanctuary as the location of subsidiary structures of the sanctuary is clear. To enable a better study and recording of the archaeological site of Amyklaion, the use of various types of digital technologies has begun in recent years, which have provided important information and results. In 2015, geodetic techniques and methods were used to investigate the area under expropriation. The space was examined using magnetic and electrical techniques with ground-penetrating radar (GPR) in order to 1) map the subsoil and identify any ancient monuments in it, 2) to calculate the exact depth at which the monuments are buried and 3) to integrate the resulting data into a GIS system¹⁶. In 2017, the entire area was mapped with 3D scanning ground-based laser scanning (TLS) using the Global Navigation Satellite System (GNSS)¹⁷.

To come to a better understanding of the abovementioned aspects, the immediate surroundings of the sanctuary were chosen in 2022 for archaeological investigations using the non-invasive archaeometric methods of geophysical prospection and remote sensing technology. The current research is based on the project »Archaeological-Geophysical prospection at the sanctuary of Apollo Amyklaios near Sparta«, which is co-financed by the »Programme for the Promotion of the Exchange and Scientific Cooperation between Greece and Germany«, under the call IKYDA 2022¹⁸. The aims of the project and the measurements were:

1) To identify further anthropogenic structures in the immediate vicinity to discuss the question of possible secondary sanctuary structures, such as stoai, hostels, cisterns, etc. and to possibly pursue them with targeted excavations.

2) To come to a better understanding of the embedding of the sanctuary in its local, regional and possibly supra-regional environment by identifying infrastructural remains.

In terms of remote sensing, the aim in 2022 was to obtain a digital elevation model of the whole archaeological site using aerial photogrammetry and LiDAR technology. Using geophysical methods, we explored the areas immediately adjacent to the sanctuary in the south (ca. 7500 m²) and west (ca. 6000 m²) of Agia Kyriaki Hill using non-invasive prospection methods. The relevance of these measures results from the archaeological results of the excavations of 2015–2022. It is the aim of this report to present the 2022 results of the geophysical and remote sensing data¹⁹. A report with an archaeological discussion and contextualization of the findings will be published after the second year (2023) of the project.

¹⁶ The GIS database of the Amykles Research project was created and is maintained by Nicola Nenci. The authors would like to thank him sincerely for discussions and the support in the contextualization of the data.

¹⁷ Responsible for the investigation in 2015 was Dr. L. Polymenakos and in 2015 Prof. V. Pagounis.

¹⁸ Collaborating Institutions: Ionian University and University of Münster.

¹⁹ Please note that only grayscale images are printed here. Colour images will be available in the online repository Zenodo.

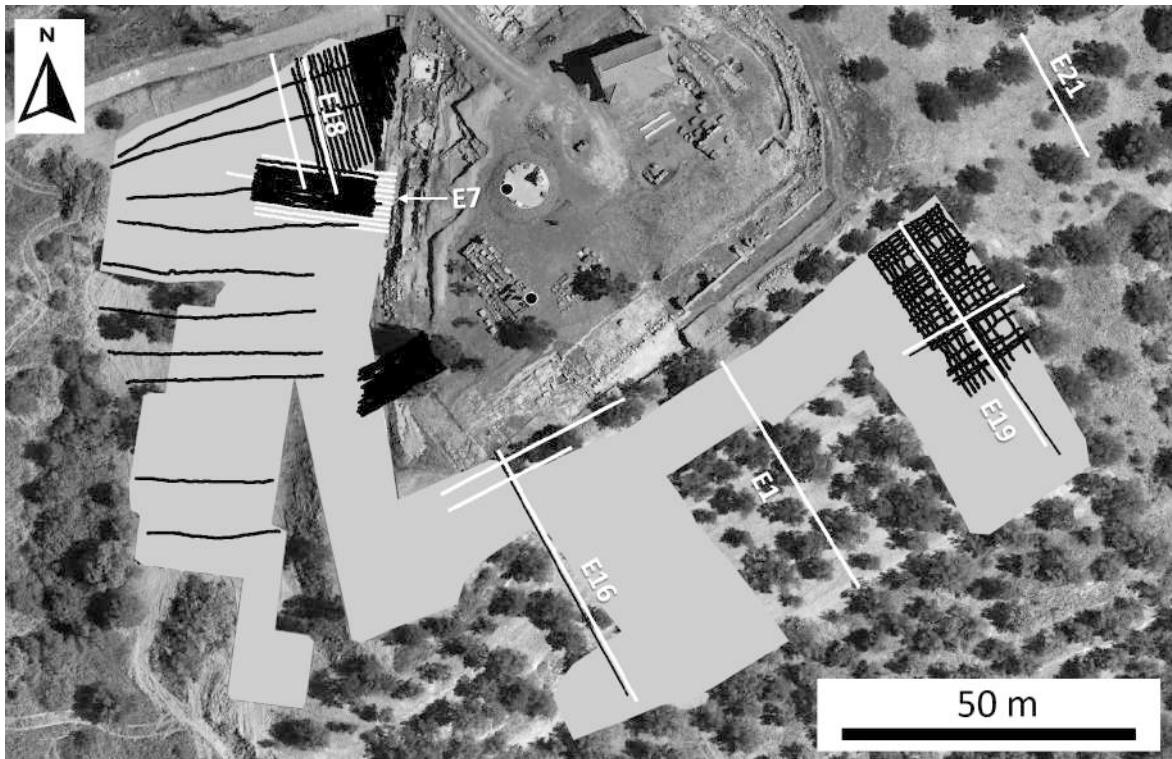


Fig. 3: Orthophoto of the investigation area showing the location of geophysical measurements. The magnetic survey was conducted in the grey filled area, black and white lines indicate GPR and ERT profiles, respectively. (Graphics: Volkmar Schmidt, Basemap photo: Amykles Research Project)

GEOPHYSICAL SURVEY

METHODS

Geophysical measurements allow for acquiring information about the subsurface in a non-invasive manner. Therefore, geophysical investigations are preferably done in the early stage of an archaeological field project. Although the measurements often give ambiguous results, they can help to develop an optimal excavation approach. At the Amyklaion, there has been sparse previous knowledge of the study site in terms of geological structure and petrophysical properties, as well as location and type of expected archaeological objects. Therefore, in the first campaign we used several geophysical methods to evaluate their suitability to investigate the subsurface in the area and to get an overview of the physical properties of the subsurface. The methods applied were magnetic surveying and susceptibility measurements, electrical resistivity tomography (ERT) and ground-penetrating radar (GPR). The location of all measured profiles and areas is shown in Fig. 3.

For the magnetometer survey in open terrain, we used a 3-channel fluxgate gradiometer (Foerster FEREX 4.032) with CON650 gradiometer probes. The instrument measures the difference of the vertical component of the magnetic field (vertical gradient) between two fluxgate sensors, which are situated at the top and the bottom of the probe at a distance of 65 cm. The survey resolution was 0.5 m between profiles and 0.25 m along profiles. In steep and tree-covered areas, we used a 2-channel total-field magnetometer (G858, Geometrics). The two sensors were mounted on top of each other with a separation of 1 m and the total magnetic field was measured at two levels above the ground. The vertical gradient of the total magnetic field can be calculated by subtraction of the readings of the two sensors. The instrument was carried along profiles with nominal spacing of 0.5 m, although the steep terrain and the olive trees often caused deviations from straight lines. In particular, there were numerous olive trees in the southeastern part of the site, causing gaps in the

magnetic measurements. Diurnal variations of the Earth's magnetic field were recorded at a base station with a proton precession magnetometer (G857, Geometrics). The inclination and declination of the Earth's magnetic field at the site was 53.5° and 4.7° , respectively, at the time of the survey. The magnetic susceptibility of selected samples was measured in-situ using a hand-held susceptometer (SM-30, ZH Instruments) with a sensitivity of 10^{-7} SI units.

Electrical resistivity tomography (ERT) was undertaken along numerous profiles using a switch device with 48 electrodes (IRIS Instruments). The electrode spacing was 0.5 m and 1.0 m, respectively. A small area (10 m x 24 m) was covered by parallel profiles with close separation (1 m), which allowed for a 3-dimensional data inversion. Since the ERT method has a rather long measurement duration, it was not possible to explore the entire area with it. Since there was no concrete evidence of structures in the subsurface visible at the surface, the location of the profiles was chosen to get a rough overview of the general situation of electrical resistances in the subsurface. Only profile E21 was positioned in such a way that it crossed an anomalous topographic feature that stood out in the results of the LiDAR survey²⁰.

For GPR measurements, we used a dual-frequency antenna (300/800 MHz) and a SIR-4000 console (GSSI). A differential positioning system with relative accuracy of <1 cm was used for topographical surveying. In the beginning, several 2D-profiles with wide spacing have been measured at the western and southern slope of the hill. Then, at locations with interesting features in the data, smaller areas were covered with closely spaced profiles (0.5 m spacing), to create depth-slices which allow for 3-dimensional interpretation of the data.

MAGNETIC SUSCEPTIBILITIES

Magnetic susceptibility (MS) describes the ability of materials to get magnetized under the influence of an external magnetic field. In the subsurface, all materials get magnetized by the Earth's magnetic field.

Contrasting values for the MS of different materials result in magnetization contrasts which are a common cause for magnetic anomalies that are measured in magnetic surveys²¹. Therefore, knowledge of the MS of the materials in the area helps to interpret the magnetic anomaly maps. Archaeological structures become visible as a magnetic anomaly only if they exhibit a contrast in magnetization relative to their surrounding material. The MS can be also used to characterize materials, since different rock types show often distinct ranges of values for the MS, which can be utilized e.g., for provenance analysis²².

The building structures at the Amyklaion consist volumetrically mainly of conglomerate, sandstone, limestone, and marble. Furthermore, bricks are often found, e.g., as flooring of a cistern. As a rule, however, the brick material is not present in a structural bond but loosely or as backfill. The soil outside the sanctuary consists almost everywhere of a sandy-marly material. Although we have no direct information about the composition of the deeper subsoil, it can be assumed that it consists of similar marly material. We expect that the geological conditions are comparable to those that were encountered during

²⁰ See below in this article.

²¹ Another cause for magnetic anomalies is the remanent magnetization of ferromagnetic materials.

²² Williams-Thorpe – Thorpe 1993; Dalan 2008.

measurements on the nearby Agios Vasilios hill²³.

The results of the MS measurements are shown in Table 1. The most commonly used building materials, conglomerate and limestone, have a very low MS. The values for soil are only slightly higher. Consequently, walls buried in soil would have very little negative susceptibility contrast. Since the upper soil layers generally have increased susceptibility, it is likely that the MS would begin to decrease a few decimeters below the ground surface. This would have the consequence that buried building structures of conglomerate and limestone form an even lower magnetization contrast to the surroundings and are no longer magnetically detectable.

Material	MS _{ave}	MS _{min}	MS _{max}	n
Conglomerate	0.13×10^{-3}	0.04×10^{-3}	0.27×10^{-3}	6
Limestone / Marble	0.13×10^{-3}	-0.02×10^{-3}	0.85×10^{-3}	7
Bricks	2.51×10^{-3}	1.44×10^{-3}	4.11×10^{-3}	4
Soil	0.52×10^{-3}	0.21×10^{-3}	0.69×10^{-3}	6

Table 1: Results of the magnetic susceptibility measurements. Average (MS_{ave}), minimum (MS_{min}), and maximum (MS_{max}) values for each material are given in SI units; n is number of measured samples.



Fig. 4: Pieces of brick with high magnetic susceptibility incorporated in wall structure. (Photo: Volkmar Schmidt)

²³ Polymenakos 2019; de Neef et al. 2022.

Bricks show considerably higher MS values and can therefore cause magnetic anomalies. However, they usually do not form systematic structures, but are irregularly distributed in walls (Fig. 4), used as backfill or occur as debris. In a magnetic survey, this will cause scattered anomalies. However, it cannot be ruled out that there are still brick structures in the area under investigation that generate interpretable magnetic anomalies. Brick backfills should also be magnetically visible.

From these data, it can be explained that building structures in the area around the Amyklaion are unlikely to produce significant magnetic anomalies. However, anomalies may be produced by less common materials with high MS values such as ash, ceramics, and iron objects, or by remanently magnetized materials such as furnaces.

MAGNETIC SURVEY

The magnetic survey covered most parts of the western and southern hillslope. Fig. 5 shows the map of the vertical gradient of the magnetic field. Although the fluxgate sensors and the total-field magnetometer measure different components of the magnetic field, the vertical gradients derived from both instruments are very similar and are therefore presented in the same map.

The map shows a variety of magnetic anomalies with values up to 400 nT. The highest values belong to dipole anomalies, which are probably caused by larger metallic objects or remanently magnetized objects. In addition, there are many small-sized and weak anomalies of objects which must be very close to or even on the Earth's surface and are very irregularly distributed. These are probably due to debris, which contains small metallic objects, brick fragments and pottery shards. The uneven distribution of anomalies is striking as is the fact that large areas in the west and southeast are littered with anomalies, but almost no anomalies are found in the southern and eastern parts.

Linear anomalies, that are commonly expected from walls and infrastructure, are also found (e.g., in the Southeast next to the peribolos and in the southernmost area), but they occur sporadically. In the western part, linear structures might be assumed, but these are obscured by small-scale, irregular anomalies. In such situations, it can be advantageous to measure the magnetic field at a somewhat higher altitude above ground, because the anomalies of small objects at the ground surface decay faster than those of deeper structures. Indeed, the total-field anomaly map measured with the top sensor is much less influenced by small-scale scattered anomalies (Fig. 6). In the western area, a large-scale anomaly with SW-NE and N-S striking edges becomes visible. This suggests larger structures in the subsurface. The negative anomaly at the northern edge of the area is probably caused by an iron gate nearby.

ELECTRICAL RESISTIVITY TOMOGRAPHY (ERT)

In total, 21 ERT profiles were measured. The results of a representative selection of profiles are shown in Fig. 7. In general, the electrical resistivity of the subsurface is quite low with values usually below 400 Ωm , and even below 80 Ωm at greater depth. These low values agree with the assumption, that the geological subsurface consists of marly rocks with considerable clay content. Profile E16 showed low resistivity even at the surface, although the measurements were made during very dry weather and there were very few precipitations in the weeks before²⁴.

²⁴ In the 8 weeks prior to the measurement, there was only 7mm of precipitation according to https://www.meteoblue.com/de/wetter/historyclimate/weatherarchive/lakedaimon_griechenland_253394?fcstlength=1m&year=2022&month=7.

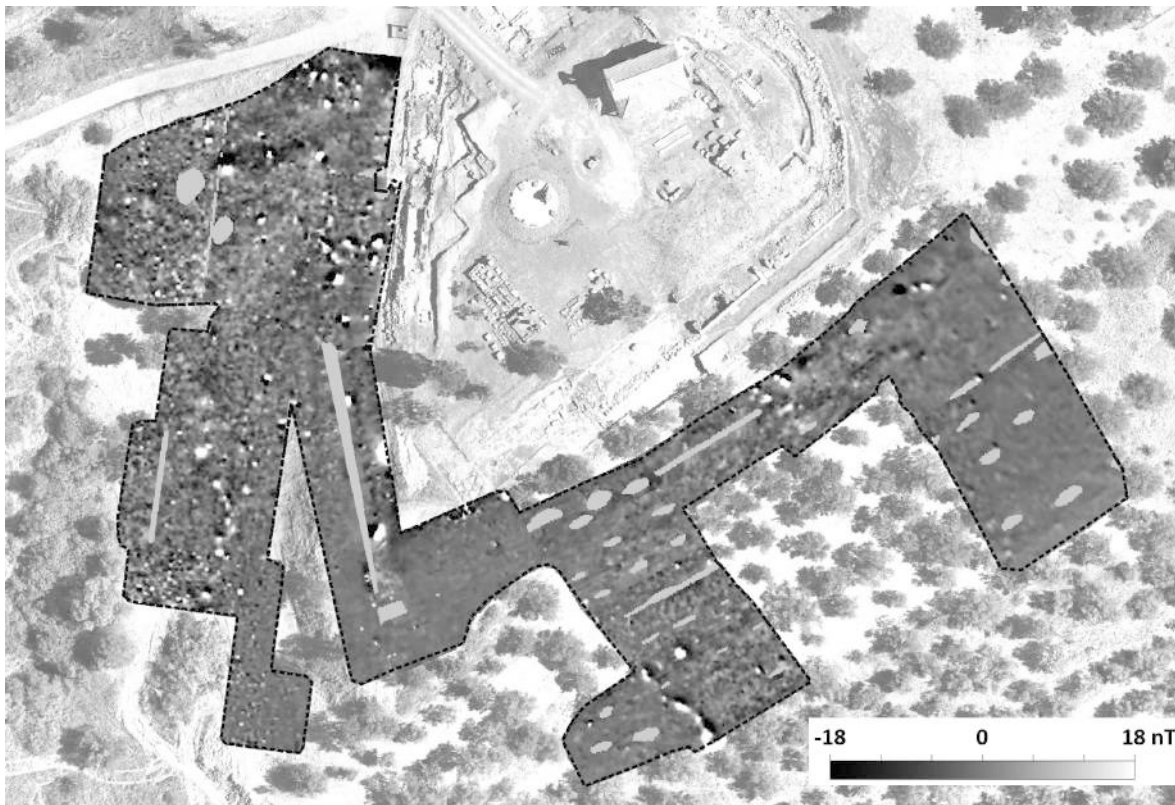


Fig. 5: Magnetic anomaly map (vertical gradient) shown on orthophoto. Value range -18 .. 18 nT (clipped). Outline of the measured area is indicated with a dashed line. Grey filled areas indicate missing data due to vegetation or steep slopes. (Graphics: Volkmar Schmidt, Basemap photo: Amykles Research Project)

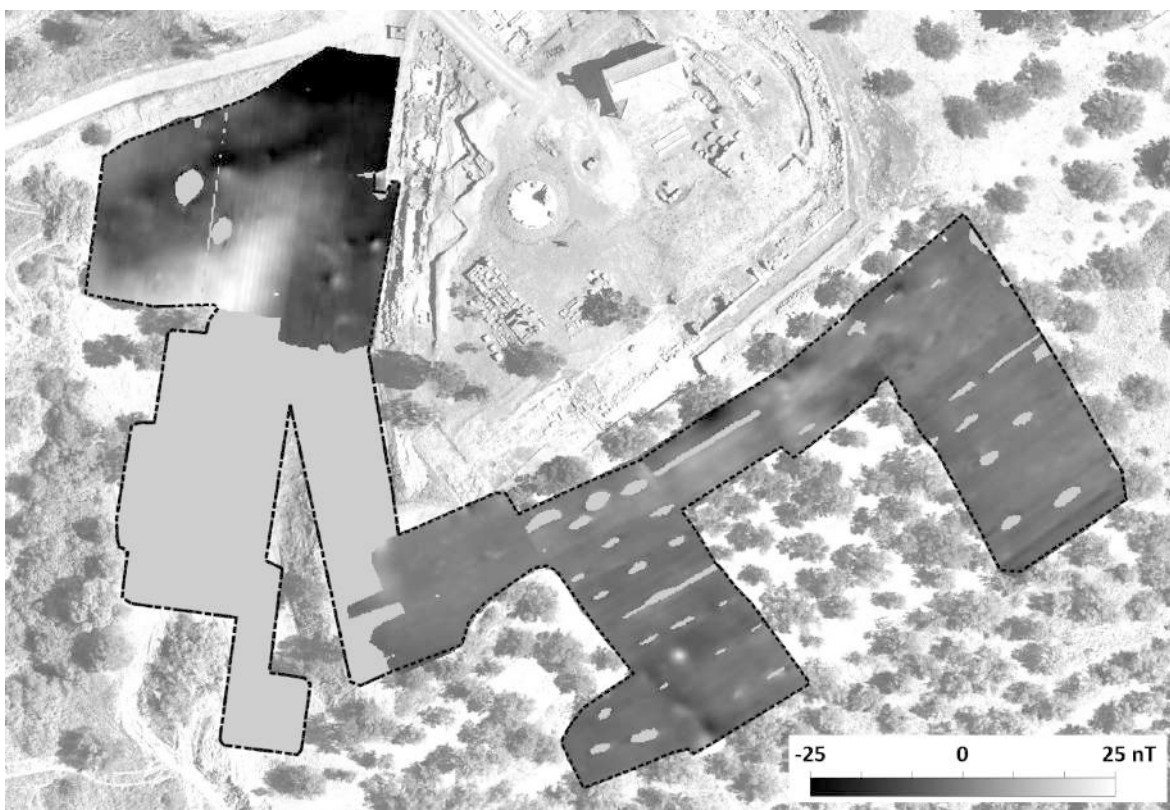


Fig. 6: Orthophoto with total-field magnetic anomaly map from top sensor. Value range -25 .. 25 nT (clipped). Outline of the measured area is indicated with a dashed line. Grey filled areas indicate missing data. (Graphics: Volkmar Schmidt, Basemap photo: Amykles Research Project)

Since common building materials at the Amyklaion such as limestone, conglomerate and bricks have higher resistivity, they are more likely to be located in areas of higher resistivity, which are found at the western slope and locally at the eastern slope. This does not rule out that in areas of low electrical resistivity, structures made of wood, clay, pits or ditches can be found.

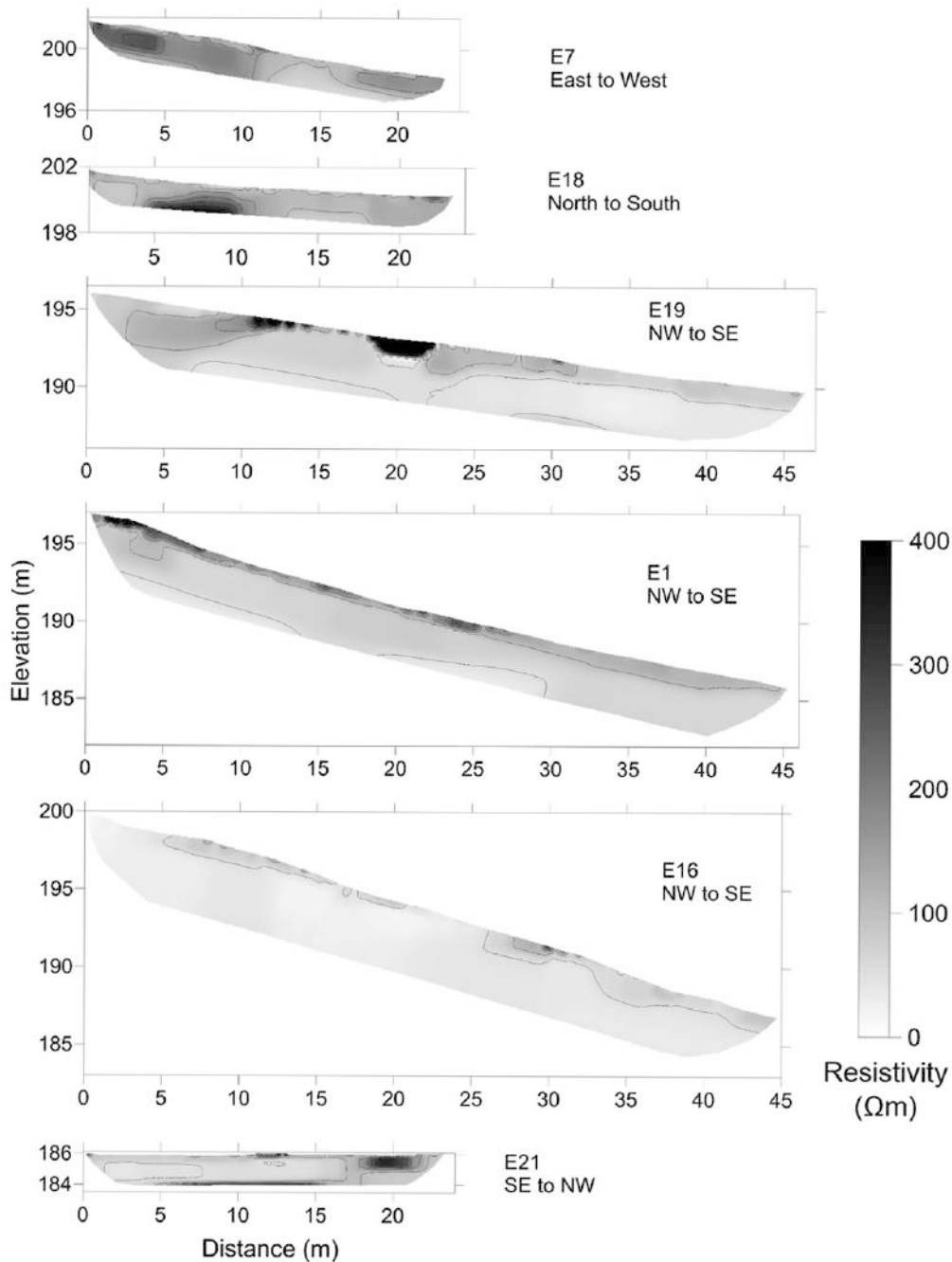


Fig. 7: Selected ERT results from: western slope (E7 and E18), southern slope (E1, E16 and E19) and eastern slope (E21). Value range 0 .. 400 Ωm (clipped). (Figure: Volkmar Schmidt)

Most profiles show intermediate resistivities close to the surface, ranging from 100 Ωm to 200 Ωm . This situation is favourable for GPR measurements, because here, radar waves can penetrate into the ground. This material is probably more sandy or gravelly and could contain pieces of hard rock or burnt bricks with high resistivity. The material could be eroded material of the conglomerate layer on top of the hill or debris from past building structures. The latter could also be relocated material from past excavations or agricultural activities. It cannot be ruled out that intercalated limestone and gravel layers, which occur in the sediments of the Spartan basin²⁵, generate intermediate and high resistivity zones. However, these layers should show a large extent and a nearly horizontal bedding. High resistivities (>300 Ωm) indicate accumulations of hard rocks or dry and porous zones. The high-resistivity zone in profile E19 at $x=20\text{m}$ reaches values of >1000 Ωm . It certainly represents an artificial accumulation of stones, which was confirmed by GPR measurements. Similar features are found in profiles E7, E18 and E21, although here, the resistivity values are lower than in profile E19. This, however, may be an effect of the data analysis, which introduces some smoothing and averaging.

Profile E7 is one of the 11 parallel, closely spaced profiles at the western slope, and it shows high-resistivity features in its eastern part close to the excavated peribolos and at the western end of the profile (Fig. 7). Looking at this profile together with the other parallel profiles gives more insight into the spatial expansion of the high-resistivity features (Fig. 8).

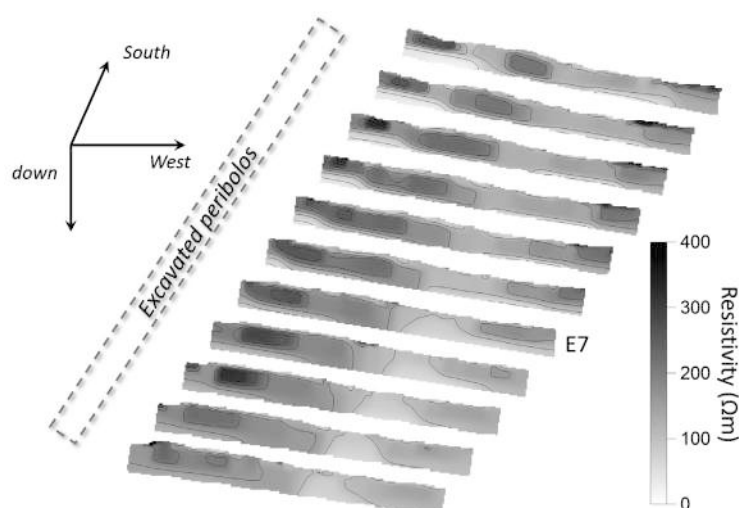


Fig. 8: Perspective view of closely spaced parallel ERT profiles at the western slope. (Figure: Volkmar Schmidt)

A high-resistivity zone is seen in the eastern part of each profile, and it is oriented parallel to the peribolos, which is situated a few meters to the East. The strike directions found in these ERT profiles correspond to the large-scale total-field magnetic anomaly (Fig. 6).

²⁵ Higgins - Higgins 1996, 52-54; Pope et al. 2003; Polymenakos 2019.

GROUND-PENETRATING RADAR (GPR)

The GPR measurements were carried out with a dual-frequency antenna. Since the data of the low-frequency antenna showed more noise and no greater penetration depth than the high-frequency antenna, only the data from the latter was used. Some examples of GPR data are shown in Fig. 9. The radargram of profile GPR67 is representative for almost all profiles on the western slope. Down to a depth of about 50cm, it shows numerous signals, mainly of hyperbolic shape. These can be caused by small objects, such as stones, litter, or tree roots (Fig. 9, feature B). Sometimes, larger reflective structures are visible (feature A). At larger times (>10 ns), the image shows mainly long-wavelength noise and no clear reflection. Obviously, the signal is being highly damped by the low electrical resistivity of the subsurface. Among the profiles on the western slope, reflections from small objects are more frequent in the northern part. This can indicate a higher anthropogenic influence. Measurements with closely spaced profiles could help to find out if the small reflective objects form archaeologically relevant structures. Such measurements have started in some areas already (Fig. 3).

Profile GPR63 (Fig. 9) shows a measurement on ground with high electrical conductivity. The profile is coinciding with ERT profile E16. The radargram contains almost exclusively technical noise and artifacts. Only one reflection hyperbola is present (feature D), which is probably due to a tree root. This result suggests that here the subsurface was not affected by human intervention.

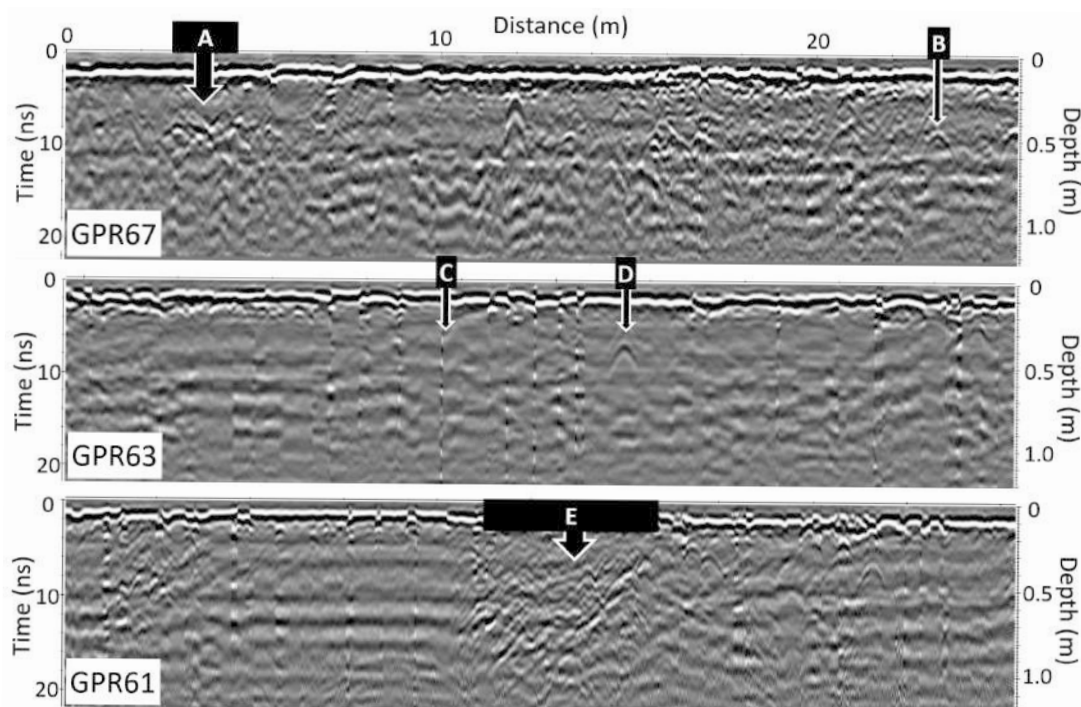


Fig. 9: Examples of GPR profile data. Depth was calculated using an assumed velocity of 0.11 m/ns.

Interpretation of selected features:

- A – reflective object at depth of ca. 40 cm,
- B and D – reflection hyperbola from small object or tree root,
- C – vertical stripe is processing artifact due to uneven ground,
- E – ca. 4 m wide zone with multiple reflections from up to 1m depth. (Figure: Moritz Wendel)

Profile GPR61 lies on ERT profile 19. It shows numerous reflections from depths up to 1m. The reflective zone E coincides with the high-resistivity feature in ERT19 (Fig. 7). The reflections could be due to remains of walls, a backfilled ditch or geological layering. In this area, multiple parallel profiles have been measured. This allows for the calculation of depth slices, i.e. maps that show the intensity of the reflections at a certain depth level below ground. The depth slices clearly show a continuation of feature E on parallel profiles and a nearly linear, north-south striking structure becomes visible (Fig.10).

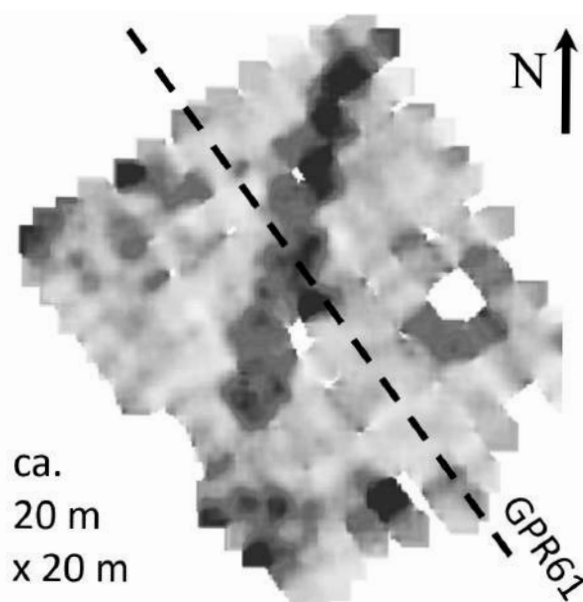


Fig. 10: GPR depth slice, 44 cm below ground. The dashed line shows the location of profile GPR61. (Figure: Volkmar Schmidt)

DISCUSSION OF GEOPHYSICAL RESULTS

These first results show that all applied geophysical methods give some valuable information about the subsurface of the Agia Kyriaki Hill. We could find regular subsurface structures and identify areas with a large density of subsurface heterogeneities, which reflect human activities.

Although magnetic surveying can cover a large area quickly, the method is not able to image all important features. For instance, the structure shown in Fig. 10 is not visible in the magnetic anomaly maps. At the western slope, the magnetogram is disturbed by a superficial debris layer, which also contains modern metal litter and obscures possible deeper structures. The measurement of the magnetic total-field anomalies at higher altitude is in this case effective to identify signals from deeper-lying structures.

The application of several methods is inevitably needed to get a complete insight into the subsurface. GPR was found to be very successful in imaging the uppermost layer, that probably contains most structures of archaeological interest. However, a dense, area-wide prospection is quite time consuming. ERT can also image relevant structures, but it lacks the resolution needed to image individual objects and walls. It allows, however, a deeper look into the subsurface. This could be helpful to identify how archaeological structures correspond with the geological conditions at the site.

To interpret the results of all geophysical and remote-sensing methods, integration of all data into a spatially consistent reference frame would be needed. Since all data is geo-referenced with an accuracy of few centimeters, this integration is possible. This would allow, for instance, to correlate small objects detected with GPR and magnetics.

LiDAR

METHODS

Aerial surveying techniques were used to provide detailed interpretation of the surface of the study area, Agia Kyriaki Hill, where the monumental Throne of Apollo is situated as well as the surrounding area. The methodology used includes the combination of close-range aerial photogrammetry²⁶ and LiDAR scanning (also known as airborne laser scanning or ALS) resulting in the production of a high resolution orthomosaic and digital surface model. Aerial photography and scanning of the area with Light Detection and Ranging (LiDAR) was carried out using an Unmanned Aircraft System (UAS) with two different payloads, specifically, the DJI Matrice 300 RTK quadcopter equipped with the Zenmuse P1 camera and the Zenmuse L1 LiDAR. For the georeferencing of the data, the RTK unit of the UAV was used, as for the more accurate georeferencing of the point cloud data of both methods, a GNSS receiver was used to survey seven (7) control points in the area.

Aerial LiDAR scanning is a remote sensing technology that uses laser light to measure distances between the sensor and the target area on the ground. The sensor emits rapid pulses of laser light and records the time it takes for the light to return from the ground surface, creating 3D point clouds. The orthomosaic is a photogrammetrically orthorectified image product mosaicked from an image collection, where the geometric distortion has been corrected and the imagery has been color balanced to produce a seamless mosaic dataset.

One significant factor affecting the final results is the accuracy of the Inertial Navigation System (INS) which is a navigation system that uses accelerometers and angular velocity meters to estimate the position, velocity, and attitude of a moving object. The DJI Zenmuse L1 INS's accuracy for yaw is 0.3° (RMS 1σ)²⁷ in real-time and 0.15° (RMS 1σ) in post-processing. Similarly, the accuracy for pitch and roll is 0.05° (RMS 1σ) in real-time and 0.025° (RMS 1σ) in post-processing, indicating that the INS can estimate the pitch, roll and yaw angles of the object with high accuracy.

The L1's Livox LiDAR module captured precise point cloud data, penetrating through the vegetation, capturing points on the ground, to create a dense and highly accurate map of the site. Meanwhile, the P1's high-resolution camera and 3-axis stabilized gimbal allowed for the capture of detailed images from multiple angles, resulting in a highly detailed and accurate orthomosaic of the area. The L1's LiDAR module can capture data with a vertical accuracy of up to 5 centimeters and a horizontal accuracy of up to 10 centimeters, while the P1's 45-megapixel full-frame sensor captures highly detailed images with exceptional color accuracy and low noise, achieved a Ground Sample Distance (GSD) of 0.75 cm per pixel at a flight altitude of 60 meters. Both sensors also feature advanced synchronization technology, ensuring accurate geotagging of captured data. The selection of those modules in the Amykles case study was based on the morphology of the surrounding terrain and the necessary vegetation removal required for the final maps.

²⁶ Panagiotidis – Zacharias 2021.

²⁷ The accuracy was measured under the following conditions in a DJI laboratory environment: after a 5-minute warm up, using Mapping Mission with Calibration Flight enabled in DJI Pilot, and with the RTK in FIX status. The relative altitude was set to 50 m, flight speed to 10 m/s, gimbal pitch to -90° , and each straight segment of the flight route was less than 1000 m. DJI Terra was used for post-processing.

For the purpose of photogrammetry and LiDAR scanning, four flights were conducted at an altitude of 60 meters above ground level while following the terrain. Specifically, two flights were carried out utilizing the Zenmuse P1 camera, and two additional flights were carried out using the Zenmuse L1 LiDAR. The P1 camera resulted in the capture of 1244 photos to facilitate mapping of the area, while the LiDAR scanning resulted in the creation of a single point cloud of 446,617,649 points. The georeferenced dense point cloud generated by the L1 scanner was pre-processed by the software DJI Terra and then by ArcGIS Pro software. During the first stage of processing, point cloud classification was employed to clear and extract ground elements. The key output of this process was the digital terrain model (DTM), which is shown in Fig. 12. All data collected was conducted using the Greek projection system GGRS '87. Regarding photogrammetry data processing, specialized software dedicated to unmanned aerial systems (UAS) mapping was used to create a georeferenced dense point cloud. Specifically, Agisoft Metashape photogrammetry software was used to produce the orthomosaic, which is shown in Fig. 11, utilizing the point cloud data. The complete orthomosaic is a high-resolution georeferenced aerial photo (107216 x 96096 pixels) with the true color of the surveyed area²⁸. By comparing the orthomosaic with the DTM visualization, changes in the terrain can be accurately identified and documented.

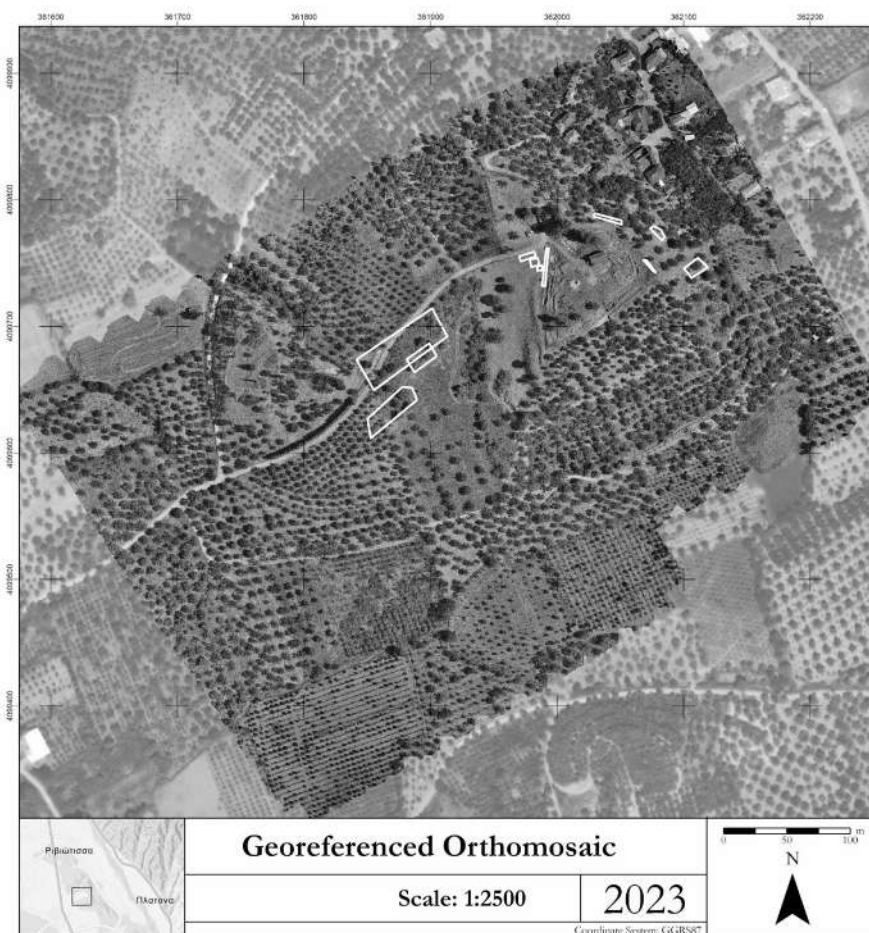


Fig. 11: Georeferenced high-resolution orthomosaic in ArcGIS environment. (Laboratory of Archaeometry, University of the Peloponnese)

²⁸ Kompoti et al. 2023.

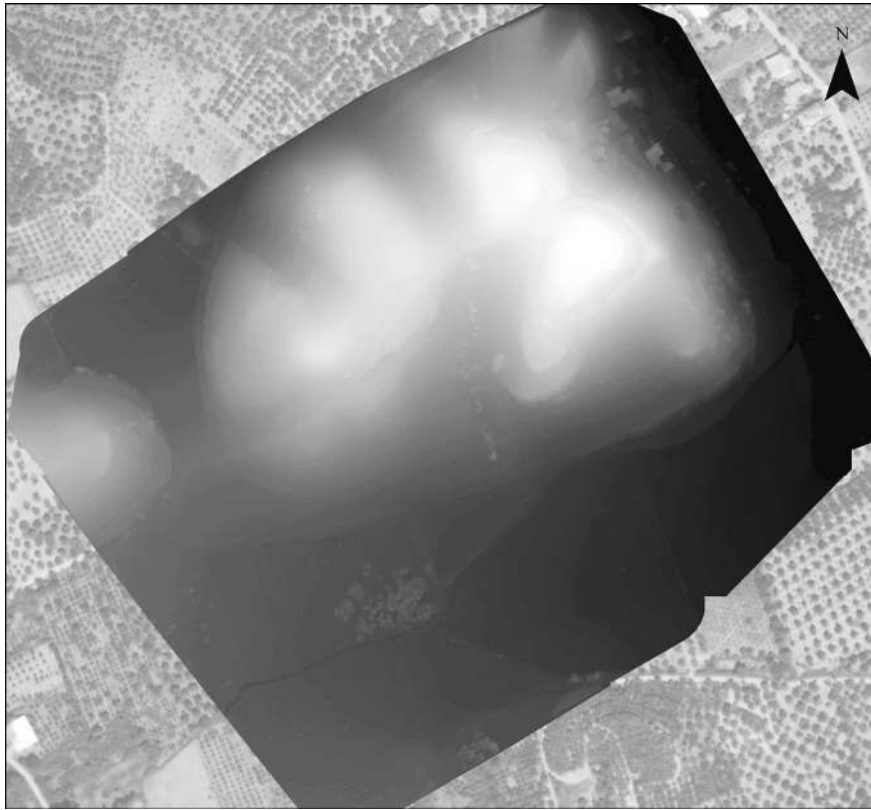


Fig. 12: Digital Terrain Model (DTM) Scale 1:2500. (Laboratory of Archaeometry, University of the Peloponnese)

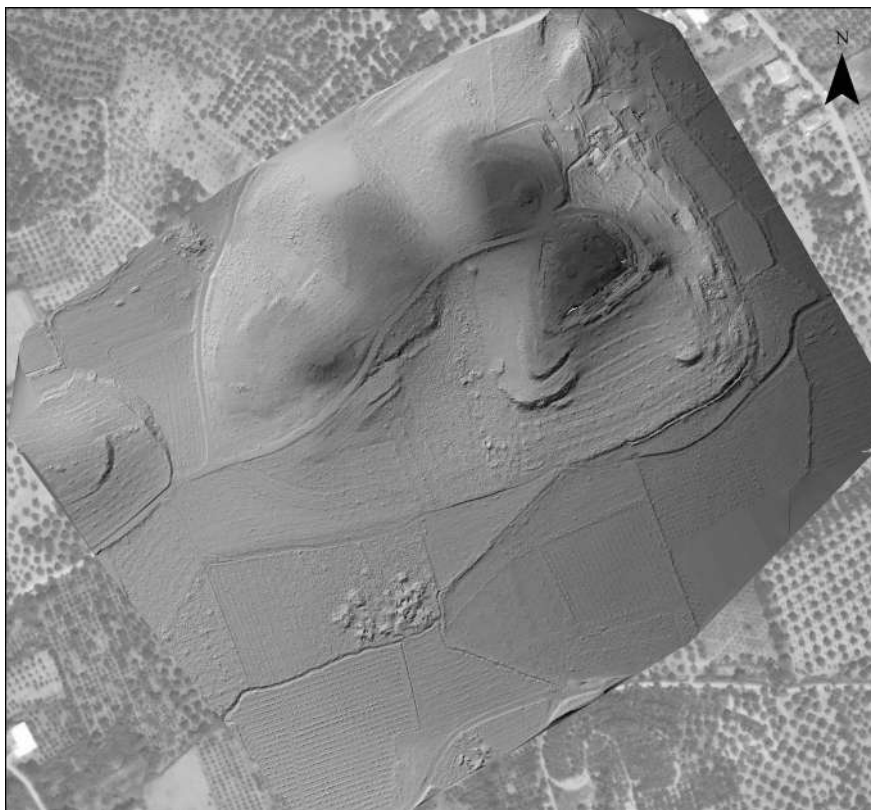


Fig. 13: Shaded Relief map Scale 1:2500. (Laboratory of Archaeometry, University of the Peloponnese)



Fig. 14: Hillshade visualization Scale 1: 2500. (Laboratory of Archaeometry, University of the Peloponnese)

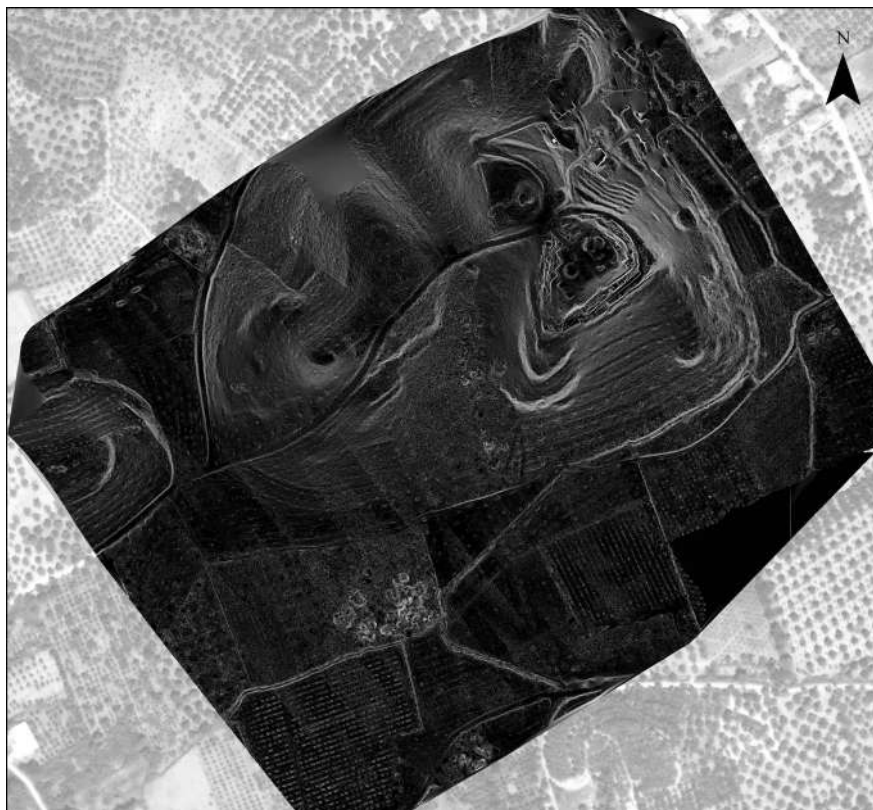


Fig. 15: Slope map Scale 1: 2500. (Laboratory of Archaeometry, University of the Peloponnese)



Fig. 16: Hillshade visualization from multiple directions Scale 1: 2500. (Laboratory of Archaeometry, University of the Peloponnese)



Fig. 17: Sky-view factor map Scale 1: 2500. (Laboratory of Archaeometry, University of the Peloponnese)



Fig. 18: Georeferenced orthophoto - POI Scale 1:750. (Laboratory of Archaeometry, University of the Peloponnese)

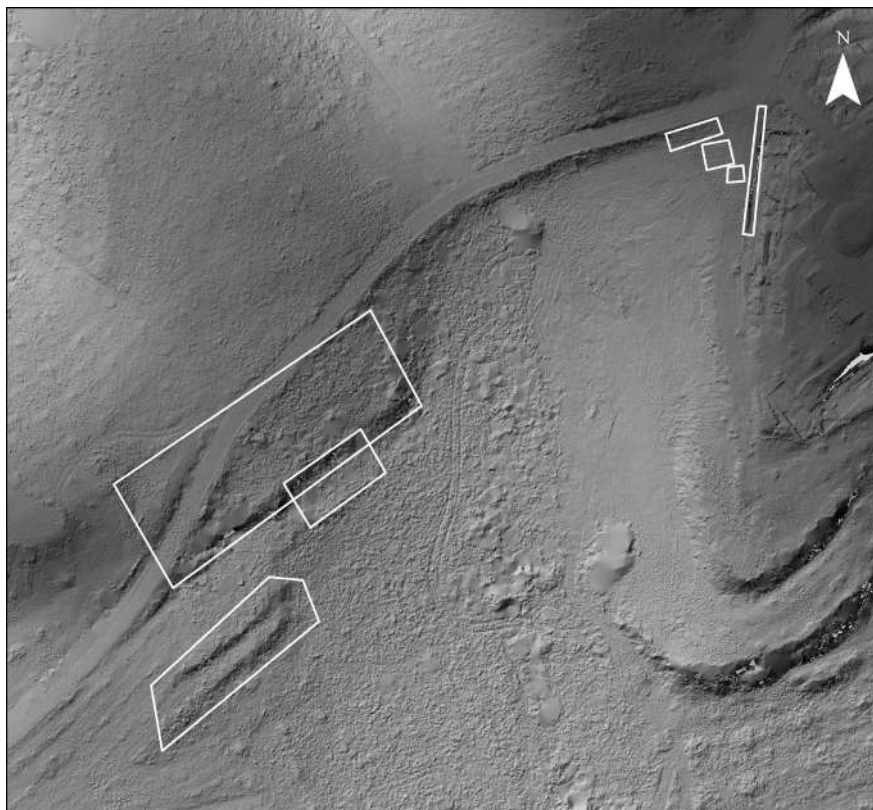


Fig. 19: Shaded Relief - POI Scale 1:750. (Laboratory of Archaeometry, University of the Peloponnese)

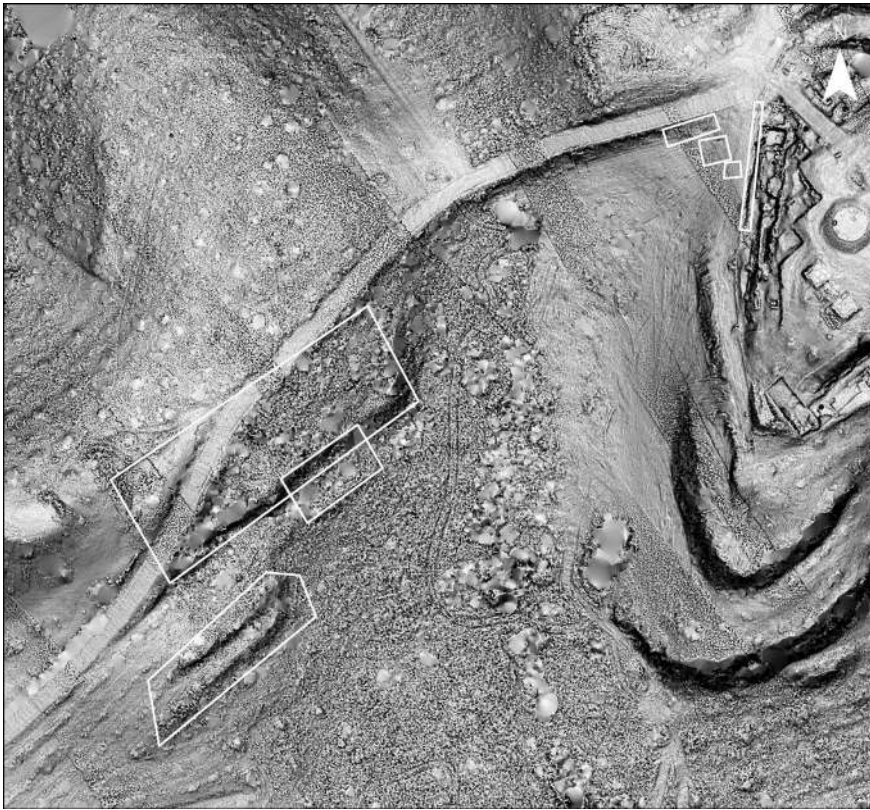


Fig. 20: Sky-View Factor 16bit - POI Scale 1:750. (Laboratory of Archaeometry, University of the Peloponnese)

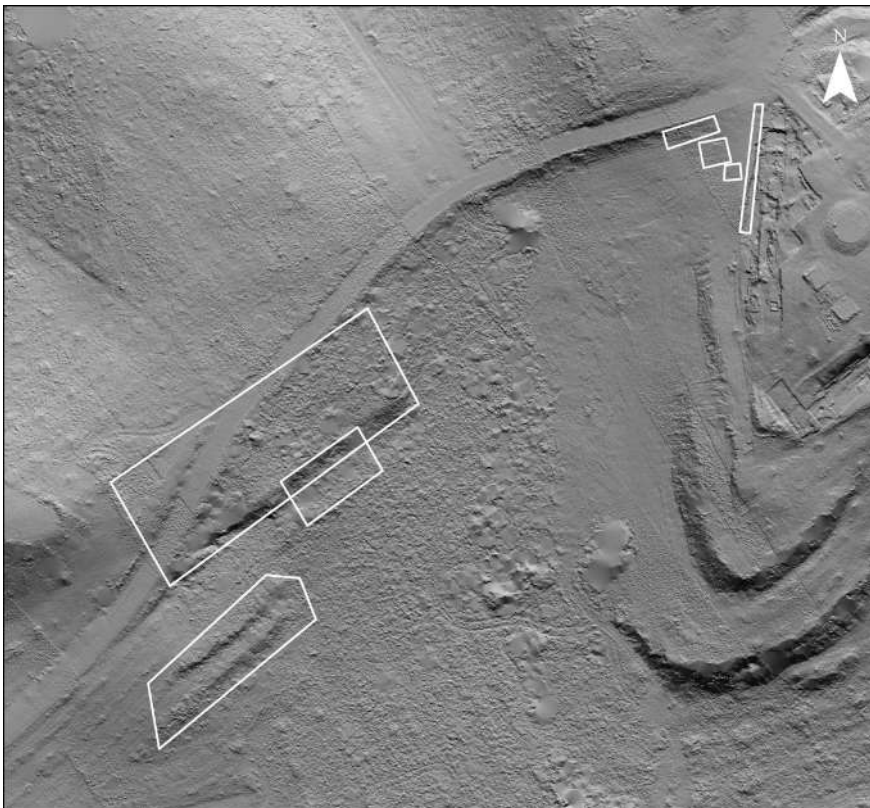


Fig. 21: Hillshading from multiple directions - POI Scale 1:750. (Laboratory of Archaeometry, University of the Peloponnese)



Fig. 22: Georeferenced orthophoto - POI Scale 1:500. (Laboratory of Archaeometry, University of the Peloponnese)

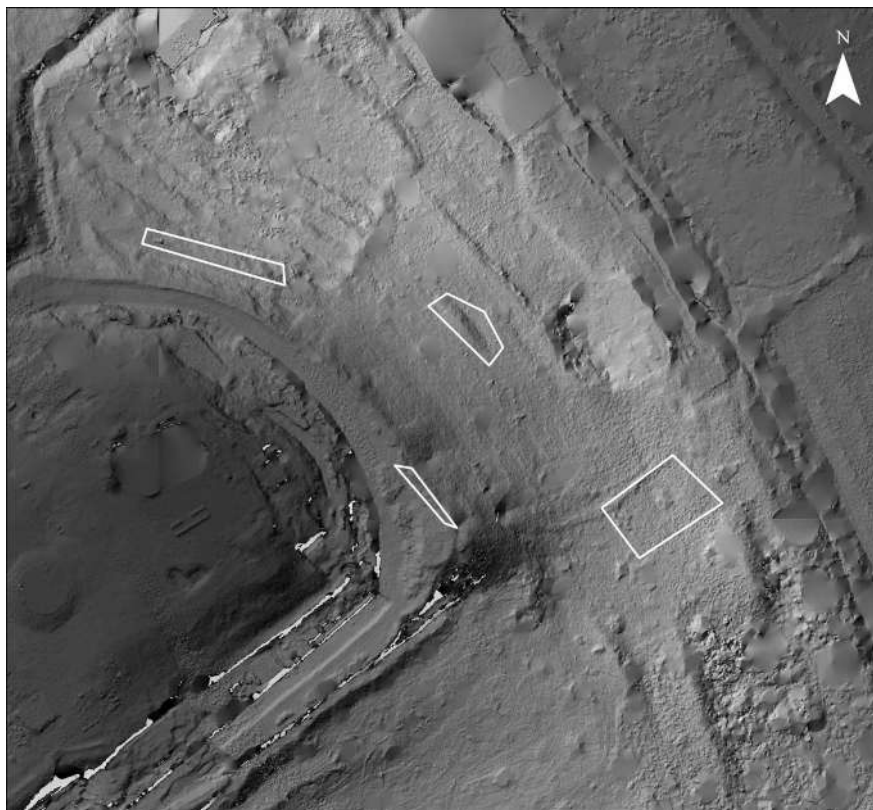


Fig. 23: Shaded Relief - POI Scale 1:500. (Laboratory of Archaeometry, University of the Peloponnese)



Fig. 24: Sky-View Factor 16bit - POI Scale 1:500. (Laboratory of Archaeometry, University of the Peloponnese)



Fig. 25: Hillshading from multiple directions - POI Scale 1:500. (Laboratory of Archaeometry, University of the Peloponnese)

RESULTS

The level of detail of the generated DTM depends on the density of the points in the scan. In the case of an archaeological site study, a greater density of ground points is required. The use of the Zenmuse L1 LiDAR and ArcGIS Pro software for point cloud classification and DTM generation is a highly effective approach in accurately capturing and analyzing the terrain of a surveyed area. By employing various filters, including noise, classification, and ground classification filters, vegetation points removed, and ground elements isolated and extracted to produce a highly accurate and detailed DTM²⁹.

The resulting DTM provides a clear picture of the variations in elevation of the surveyed area, highlighting any changes in terrain. The accuracy of the DTM can be evaluated through cross-validation with GCPs and visual inspection, which demonstrate a high degree of accuracy and precision, with a root mean-square error (RMSE) of less than 5 cm. The Shaded Relief map is a visualization tool that provides a three-dimensional representation of the terrain and contours as shown in Fig. 13. This map simulates the shadows and highlights that would be created by a hypothetical light source, creating a realistic and accurate depiction of the surveyed area, revealing features with low light source on flat areas such as in the case of the recently cleared area west of the peribolos.

RVT (Relief Visualization Toolbox) 2.2.1, a software tool used for visualizing digital terrain models (DTMs) was used for the further examination of the study area. Initially, the DTM created from the point cloud classification process is imported into RVT 2.2.1. Once imported, various visualization techniques are applied to the DTM to highlight specific features and characteristics such as Hillshade, Slope maps, Sky View factor and Multidirectional Hillshade. Hillshade, a 3D representation of the terrain, with light sources used to create shadows that help highlight subtle variations in elevation is the most commonly used visualization for interpretation of microrelief structures³⁰. This technique is especially useful for highlighting the topography of the surveyed area and identifying any features (Fig. 14). Another technique that was applied to the DTM is slope mapping. Slope maps use color gradients to represent the degree of slope in different areas of the terrain. This technique can be useful for identifying areas with steep slopes or changes in elevation (Fig. 15). Sky-view factor mapping refers to the proportion of the visible sky in a particular location by using color gradients to represent the amount of visible sky in different areas of the terrain. This technique can be useful for understanding the amount of solar radiation that different areas receive (Fig. 17). In order to overcome the directional problems of hill-shading sky-view factor can be used as an alternative method of relief mapping³¹. Another RVT tool that was used in that project is hillshading visualization from multiple directions, which creates detailed and shaded representation of the terrain as shown in Fig. 16³².

²⁹ Štular et al. 2021.

³⁰ Kokalj – Hesse 2017.

³¹ Kokalj et al. 2011.

³² Monterroso-Checa et al. 2021.

Points of interest can be identified based on the above visualizations. Highlighted for the purposes of this initial presentation are the positions NE and SW of the hill. Variations in the terrain depending on the visualization method show anomalies created from features which can be resulting from structures or remains on the ground not visible due to vegetation or features close to the surface which create slight changes in the slope.

Specifically, south west of the peribolos two outlines are accountable which are suggested for further research using geophysical methods (Fig. 18- Fig. 21). This location coincides with surface evidence which remains to be determined by further investigation. Similarly, north east of Agia Kyriaki Hill positions which show variations in their representations have been signified (Fig. 22- Fig. 25). The data sources will be further analyzed using additional visualization techniques such as PCA of hillshadings for 16 different directions.

DISCUSSION / HYPOTHESES OF THE AERIAL SURVEY TECHNIQUES

Airborne laser scanning in combination with high-resolution close-range photogrammetry have proven to give valuable results in the investigation of the sites of archaeological interest such as Agia Kyriaki hill study area. The visualization filters used on the DTM offered several points of potential archaeological significance for further investigation. The combination of data from the airborne laser scans with high resolution photogrammetry create a detailed and accurate picture of the site, which can help guide further non-destructive investigation and subsequently to better targeted excavation.

For a better evaluation of the data and results of all methods used will be integrated to a unified georeferenced database in different layers. The different layers in the database can be used to represent different aspects of the data, such as the topography of the hill, the identification of potential archaeological sites, and the results of the geophysical surveys. By combining and visualizing the data in this way, it will be possible to identify patterns and relations between different aspects of the data, providing valuable insights into the cultural and historical significance of the archaeological site.

In conclusion, the geophysical survey in combination with aerial conducted at the Amykles case using a combination of aerial photogrammetry and LiDAR scanning has provided valuable information about the subsurface features of the area. The resulting data sets have allowed for the creation of accurate and detailed 3D models and maps, which have determined possible positions of interest on the ground. The proposed positions for further geophysical investigations have the potential to uncover significant cultural heritage resources, providing a deeper understanding of the history and development of the site. The SW and NE parts of the hill have been identified as areas of particular interest and are proposed to be investigated further using geophysical methods.

CONCLUSION

For the first time in 2022, research at the sanctuary of Apollo Amyklaios in Sparta turned exclusively to the use of technologies for the exploration of the subsurface with non-invasive methods. The occasion and aim of these interventions were to investigate the hypothesis of possible constructions outside the main sanctuary defined by the enclosure, since it is known that ancient Greek sanctuaries sometimes incorporated areas directly adjacent to the main site. Specifically, for the Amyklaion, assumptions can be made about the existence of infrastructure such as dining and accommodation areas, as well as facilities for sports competitions as it is known that in the context of the Hyakinthia festival, sports competitions

were held along with musical and theatrical performances.

Our findings provide evidence for the use of the adjacent areas of the sanctuary, i. e. outside the peribolos. In the magnetometry, this is indicated by the high density of anomalies especially in the western and in parts of the southern slopes of the hill. A large curvilinear magnetic anomaly suggests unusual anthropogenic activity in the southwestern part of the south slope. The results obtained by the ERT and GPR measurements are consistent with the conclusion drawn from the magnetometry results insofar as the west and south slopes of Agia Kyriaki Hill show signs of anthropogenic use, but they do not yet allow any further conclusions to be drawn about the type of use. However, large building structures close to the surface can be ruled out in the areas investigated. Variations in the terrain as obtained by the LiDAR scanning may also be related to human activity during the long history of the site. Contrary to our expectations, the results of the magnetometry survey yielded no proof of architectural structures in these areas. This absence of evidence does not, however, necessarily mean evidence of absence, since, as described above, the building materials at the Amyklaion do not possess an increased magnetization. A possible explanation might also be that architectural remains are covered by layers of debris accumulated over the centuries. Some of this debris might even originate from past excavations which have used these areas as a dump.

Although at present we are not in the position to determine the extent to which the hill slopes were used let alone discuss the chronology, the results obtained by the combination of the different applied methods have not only in general confirmed the anthropogenic use of the hill slopes but also allowed us to identify potential areas of interest such as the curvilinear anomaly in the southeast of the hill. These can now be targeted by archaeological excavations starting in 2023 with the aim of gaining a better understanding of the use of the adjacent areas of the sanctuary of Apollon Amyklaios.

BIBLIOGRAPHY

- Bilis – Magnisali 2011–2012 T. Bilis. – M. Magnisali, Issues Concerning the Architectural Reconstruction of the Monuments of the Sanctuary of Apollo Amyklaios, in: Mouseio Benakē. The Annual Journal of the Benaki Museum 11–12, 2011–2012, 125–136.
- Brulé 1992 P. Brulé, Fêtes grecques: Périodicité et initiations. Hyakinthies et Panathénées, in: A. Moreau (ed.), L'initiation. Les rites d'adolescence et les mystères I. Actes du colloque international de Montpellier 11-14 Avril 1991 (Montpellier 1992).
- Buschor – von Massow 1927 E. Buschor – W. von Massow, Vom Amyklaion, AM 52, 1927, 1–85.
- Calame 1997 C. Calame, Choruses of Young Women in Ancient Greece: Their Morphology, Religious Role, and Social Function (Lanham 1997).
- Dalan 2008 R. A. Dalan, A Review of the Role of Magnetic Susceptibility in Archaeogeophysical Studies in the USA: Recent Developments and Prospects, Archaeological Prospection 15, 2008, 1–31, <https://doi.org/10.1002/arp.323>.
- Dalan 2017 R. A. Dalan, Susceptibility, in: A. S. Gilbert (ed.), Encyclopedia of Geoarchaeology. Encyclopedia of Earth Sciences Series (Dordrecht 2016) 939–943, https://doi.org/10.1007/978-1-4020-4409-0_170.
- de Neef et al. 2022 W. de Neef – S. Voutsaki – B. Ullrich – R. Freibothé, A palace under the olive trees. Investigating the spatial organization of the Mycenaean palatial center at Ayios Vasileios (Laconia, Greece) through large-scale magnetic gradiometry, Archaeological and Anthropological Sciences 14, 34, 2022, <https://doi.org/10.1007/s12520-022-01513-6>.
- Delivorrias 2009 A. Delivorrias, The Throne of Apollo at the Amyklaion. Old Proposals, New Perspectives, in: W. G. Cavanagh – C. Gallou – M. Georgiadis (eds.), Sparta and Laconia, from Prehistory to Premodern. Proceedings of the Conference, 17–20 March 2005, Sparta, British School at Athens Studies 16 (London 2009) 133–135.
- Demakopoulou 1982 K. Demakopoulou, Το Μυκηναϊκό Ιερό στο Αμυκλαίο και η ΥΕΙΠΓ περίοδος στη Λακωνία (PhD University of Athens 1982).
- Demakopoulou 2009a K. Demakopoulou, Το Μυκηναϊκό Ιερό Στο Αμυκλαίο: Μια Νέα Προσέγγιση, in: W. G. Cavanagh – C. Gallou – M. Georgiadis (eds.), Sparta and Laconia, from Prehistory to Premodern. Proceedings of the Conference, 17–20 March 2005, Sparta, British School at Athens Studies 16 (London 2009) 95–104.
- Demakopoulou 2009b K. Demakopoulou, Laconia in LH III C Late and Submycenaean: Evidence from Epidauros Limera, Pellana, the Amyklaion and other Sites, in: S. Deger-Jalkotzy – A. E. Bächle (eds.), LH III C chronology and synchronisms III : LH III C Late and the transition to the early iron age : proceedings of the International workshop held at the Austrian Academy of Sciences at Vienna, February 23rd and 24th, 2007 (Vienna 2009) 117–132.

- Demakopoulou 2011–2012 K. Demakopoulou, The Early Cult at the Amyklaion. The Mycenaean Sanctuary, in: Mouseio Benakē. The Annual Journal of the Benaki Museum 11–12, 2011–2012, 105–112.
- Fiechter 1905 E. Fiechter, Amyklæ. Der Thron des Apollon, *JdI* 33, 107–245.
- Förtsch 2001 R. Förtsch, Kunstverwendung und Kunstlegitimation im archaischen und frühklassischen Sparta (Mainz am Rhein 2001).
- Higgins - Higgins 1996 M. D. Higgins – R. Higgins, A Geological Companion to Greece and the Aegean (Ithaca 1996).
- Kokalj – Hesse 2017 Z. Kokalj – R. Hesse, Airborne laser scanning raster data visualization: A Guide to Good Practice (Ljubljana 2017) 16–22. 48.
- Kokalj et al. 2011 Z. Kokalj – K. Zaksek – K. Oštir, Application of sky-view factor for the visualization of historic landscape features in lidar-derived relief models, *Antiquity* 85, 2011, 263–273.
- Kompoti et al. 2023 A. Kompoti – A. Kazolias – V. V. Panagiotidis – N. Zacharias, 3D Laser Scanning and UAVs in cultural heritage. The case of Old Navarino castle in Pylos, Greece, *Journal of Archaeological Science: Reports* 52, 2023, <https://doi.org/10.1016/j.jasrep.2023.104223>.
- Larson 2007 J. Larson, *Ancient Greek Cults. A Guide* (New York 2007).
- Martin 1987 R. Martin, Bathyclès de Magnésie et le trône d'Apollon à Amyklæ, in: R. Martin (ed), *Architecture et urbanisme*, CEFR 99 (Rome 1987) 369–387.
- Matalas 2011–2012 P. Matalas, Searching for the Amyklaion: For a History of the 'Discovery' of the Sanctuary in the Modern Era, in: Mouseio Benakē. The Annual Journal of the Benaki Museum 11–12, 2011–2012, 169–178.
- Monterroso-Checa et al. 2021 A. Monterroso-Checa – J. C. Moreno-Escribano – M. Gasparini – J. A. Conejo-Moreno – J. L. Domínguez-Jiménez, Revealing Archaeological Sites under Mediterranean Forest Canopy Using LiDAR. El Viandar Castle (husum) in El Hoyo (Belmez-Córdoba, Spain), *Drones* 5, 3, 2021, 72, <https://doi.org/10.3390/drones5030072>.
- Panagiotidis – Zacharias 2021 V. V. Panagiotidis – N. Zacharias, Digital Mystras: An approach towards understanding the use of an archaeological space, *Scientific Culture* 8, 3, 2021, 89–103.
- Parker 2011 R. Parker, *On Greek Religion* (Ithaca 2011).
- Petropoulou 2015 A. Petropoulou, Hieromênia and Sacrifice during the Hyakinthia, *Mètis* 13, 2015, 167–188.

- Petterson 1992 M. Petterson, *Cults of Apollo at Sparta. The Hyakinthia, the Gymnopaïdai and the Karneia*, *Skrifter utgivna av Svenska Institutet i Athen* 8, 12 (Stockholm 1992).
- Polymenakos 2019 L. Polymenakos, Searching for prehistoric small-sized graves in complex geoarchaeological conditions. Ayios Vasilios North Cemetery (Peloponnese, Greece), *Journal of Archaeological Science* 24, 2019, 1–15.
- Pope et al. 2003 R. J. J. Pope – K. N. Wilkinson – A. C. Millington, Human and climatic impact on late Quaternary deposition in the Sparta Basin Piedmont: Evidence from alluvial fan systems, *Geoarchaeology* 18, 7, 2003, 685–724, <https://doi.org/10.1002/gea.10089>.
- Prost 2018 F. Prost, *Laconian Art*, in: A. Powell (ed.), *A Companion to Sparta I* (Hoboken 2018) 154–176.
- Richer 2012 N. Richer, *La religion des Spartiates. Croyances et cultes dans l'Antiquité*, *Histoire* 113 (Paris 2012).
- Rolley 1977 C. Rolley, *Le problème de l'art laconien*, *Ktéma* 2, 1977, 125–140.
- Štular et al. 2021 B. Štular – E. Lozić – S. Eichert, Airborne LiDAR-Derived Digital Elevation Model for Archaeology. *Remote Sensing* 13, 9, 1855, <https://doi.org/10.3390/rs13091855>.
- Tsountas 1892 C. Tsountas, *Ἐκ τοῦ Ἀμυκλαίου*, *AEphem*, 1892, 1–26.
- Tosti 2020 V. Tosti, *La naissance de Sparte: entre sources littéraires et sources archéologiques*, *Gaia. Revue interdisciplinaire sur la Grèce archaïque* 22-23, 2020, <https://doi.org/10.4000/gaia.839>.
- Vlachou 2017 V. Vlachou, *From Mycenaean Cult Practice to the Hyakinthia Festival of the Spartan Polis. Cult Images, Textiles and Ritual Activity at Amykles*, in: A. Tsingarida – I. S. Lemos (eds.), *Constructing Social Identities in Early Iron Age and Archaic Greece*, *Études d'archéologie* 12 (Brussels 2017) 11–42.
- Vlachou 2018 V. Vlachou, *Feasting at the Sanctuary of Apollo Hyakinthos at Amykles. The Evidence from the Early Iron Age*, in: F. van den Eijnde – J. H. Blok – R. Strootman (eds.), *Feasting and polis institutions*, *Mnemosyne: Bibliotheca Classica Batava Suppl.* 414 (Leiden 2018) 93–124.
- Vlizos 2009 S. Vlizos, *The Amyklaion Revisited. New Observations on Laconian Sanctuary of Apollo*, in: N. Kaltsas (ed), *Athens-Sparta. Contributions to the Research on the History and Archaeology of the Two City-States*. *Proceedings of the International Conference held at the Onassis Cultural Center on Saturday, April 21, 2007* (New York 2009) 11–23.

- Vlzos 2010a S. Vlzos, Ιερό του Αμυκλαίου Απόλλωνος στις Αμύκλες, *ADelt* 65, 2010, 577–579.
- Vlzos 2010b S. Vlzos, *Mouseio Benakē. The Annual Journal of the Benaki Museum* 10, 2010, 244–245.
- Vlzos 2011–2012 S. Vlzos, Amykles Research Project: Works 2005–2010, in: *Mouseio Benakē. The Annual Journal of the Benaki Museum* 11–12, 2011–2012, 91–104.
- Vlzos 2017 S. Vlzos, Das Heiligtum und seine Weihgaben. Bronzestatuetten aus dem Amyklaion, in: H. Frielinghaus – J. Stroszeck (eds), *Kulte und Heiligtümer in Griechenland. Neue Funde und Forschungen (Möhnesee 2017)* 71–96.
- Vlzos 2019 S. Vlzos, Deutsche Archäologen und das frühe Interesse an Sparta. Furtwängler, Fiechter, Buschor, ihre Vorgänger und die Ausgrabungen im Amyklaion, in: K. Sporn – A. Kankeleit (eds), *Die Abteilung Athen des DAI und die Aktivitäten deutscher Archäologen in Griechenland 1874–1933 (Berlin 2019)* 205–218.
- Vlzos 2020 S. Vlzos, Metallwerkstätten, Produktion und Infrastruktur des Heiligtums. der Fall des spartanischen Amyklaions, in: A. Lo Monaco (ed), *Spending on the Gods. Economy, Financial Resources and Management in the Sanctuaries in Greece, ASAtene Suppl. 7 (Athens 2020)* 37–46.
- Welwei 2013 K.-W. Welwei, *Sparta. Aufstieg und Niedergang einer antiken Großmacht*³ (Stuttgart 2013).
- Williams-Thorpe – Thorpe 1993 O. Williams-Thorpe – R. S. Thorpe, Magnetic susceptibility used in non-destructive provenancing of Roman granite columns, *Archaeometry* 35,2, 1993, 185–195, <https://doi.org/10.1111/j.1475-4754.1993.tb01034.x>.

